

## Article

# Nickel-Catalyzed Ethylene Dimerization Based on PNP(NR<sub>2</sub>)<sub>2</sub> Ligands

Chengang Cao , Haonan Fan , Jingyi Zhang, Jing Ma and Tao Jiang \*

College of Chemical Engineering and Material Science, Tianjin University of Science and Technology, Tianjin 300457, China

\* Correspondence: jiangtao@tust.edu.cn

**Abstract:** Nickel (II) complexes stabilized by PNP(NR<sub>2</sub>)<sub>2</sub> (L<sup>1</sup>: R = Methyl, L<sup>2</sup>: R = ethyl, L<sup>3</sup>: R = isopropyl) ligands were synthesized and characterized. A narrow range of products was observed for catalytic systems containing nickel complexes and ethyl aluminum dichloride (EADC). All exhibit considerable activity in the ethylene dimerization to produce 1-butene. Precatalyst **1** is the most conducive for ethylene dimerization, producing 83.4% C<sub>4</sub> (1-C<sub>4</sub> 36.8%) and 103.0 × 10<sup>5</sup> g/(molNi·h) in terms of its activity under the appropriate conditions. By adjusting the conditions of the catalytic system for precatalyst **2**, high C<sub>4</sub> selectivity (88.1%) with reasonable activity (76.9 × 10<sup>5</sup> g/(molNi·h)) can be obtained. The X-ray single-crystal analysis of complexes presents mononuclear bidentate coordination at the Ni center, and the relationship between certain bite angles may also imply catalytic performance.

**Keywords:** ethylene oligomerization; nickel complex; PNP(NR<sub>2</sub>)<sub>2</sub> ligand; 1-butene



**Citation:** Cao, C.; Fan, H.; Zhang, J.; Ma, J.; Jiang, T. Nickel-Catalyzed Ethylene Dimerization Based on PNP(NR<sub>2</sub>)<sub>2</sub> Ligands. *Catalysts* **2022**, *12*, 1008. <https://doi.org/10.3390/catal12091008>

Academic Editors: Fabio Ragaini and Victorio Cadierno

Received: 4 August 2022

Accepted: 3 September 2022

Published: 6 September 2022

**Publisher's Note:** MDPI stays neutral with regard to jurisdictional claims in published maps and institutional affiliations.



**Copyright:** © 2022 by the authors. Licensee MDPI, Basel, Switzerland. This article is an open access article distributed under the terms and conditions of the Creative Commons Attribution (CC BY) license (<https://creativecommons.org/licenses/by/4.0/>).

## 1. Introduction

In recent years, nickel complexes have attracted widespread attention as transition-metal catalysts for ethylene oligomerization (especially ethylene dimerization) in academic and industrial fields [1–3]. The nickel-catalyst system can mainly generate 1-butene and 2-butene, which can be used as comonomers for butanone, polypropylene, polyethylene, and butylene oxide [4]. The catalytic process induced by a traditional nickel catalyst may produce olefin products containing only a small proportion of 1-butene (Schultz–Flory distribution), which cannot meet the high market demand for 1-butene [5]. To improve product selectivity and avoid product slate issues, nickel-catalyzed ethylene oligomerization is being increasingly studied in the literature [6–11].

The tridentate pyrazolyl ligand-based nickel complexes reported in a study by Casagrande et al. [12] obtained approximately 99% C<sub>4</sub> selectivity. Piers et al. [13] synthesized phosphino-borate ligands, in which the P and F atoms were chelated with Ni to form bidentate P<sup>+</sup>F nickel catalysts, which effectively catalyzed the oligomerization of ethylene under very mild conditions without the addition of ligand scavengers and cocatalysts. Sun et al. [14] created nickel complexes with tridentate ONS ligands that are highly active (1.4 × 10<sup>7</sup> g/(molNi·h)) in ethylene dimerization, providing up to >99% selectivity for 1-butene. It has been shown that the stereo-electronic properties of the ligand have a significant effect on the performance of the catalyst, e.g., the incorporation of different substituents or heteroatoms into their structure can significantly influence both the catalytic activity and selectivity of the ethylene oligomerization/polymerization process [10]. To further explore the role of the ligand structure in the nickel-based catalytic system, our group reports on the dimerization catalytic system based on P<sup>+</sup>SiP, P<sup>+</sup>NSiP, P<sup>+</sup>CSiP, and P<sup>+</sup>CSiCP ligands [4,15,16]. In the current study, we successfully prepared three new nickel complexes stabilized by PNP(NR<sub>2</sub>)<sub>2</sub> ligands for ethylene oligomerization, all of which present good ethylene oligomerization performances.

## 2. Results and Discussion

We investigated the catalytic performance of Ni-based  $\text{PNP}(\text{NR}_2)_2$  catalysts when activated with an EADC cocatalyst in a methylcyclohexane solvent. Furthermore, we compared the catalytic systems of precatalysts 1–3 and presented the corresponding evaluation in Table 1. It was observed that precatalyst 1 presented the greatest activity ( $103.0 \times 10^5 \text{ g}/(\text{molNi}\cdot\text{h})$ ) and  $\text{C}_4$  selectivity (84.3%) (Table 1, entry 1), slightly better than precatalyst 2 (Table 1, entry 2). Steric hindrance plays an important role in the regulation of a catalyst's performance. The percent buried volume (%Vbur) was calculated, and the corresponding steric map was created using the online tool SambVca 2.1 [17]. Precatalyst 3 (37.3%Vbur, Figure 1), with its large steric bulk, may reduce the possibility of the successful coordination of ethylene with the metal center, resulting in reduced catalytic activity [18,19]. Therefore, the catalytic systems of precatalysts 1 (28.3%Vbur, Figure 1) and 2 (33.2%Vbur, Figure 1), with fewer R-substituents in the ligands, present greater activity. Unexpectedly, precatalyst 3 did not exhibit the highest  $\text{C}_4$  selectivity when compared to precatalysts 1 and 2. This may be due to the high steric bulk of precatalyst 3, where the  $1\text{-C}_4$  released from the active center could not exit the catalytic pocket and the incoming ethylene molecule could not undergo a co-oligomerization reaction with  $1\text{-C}_4$ , resulting in a higher  $\text{C}_6$  selectivity (30.1%), which was the reason for only 0.6% of  $1\text{-C}_6$  being present in the  $\text{C}_6$  fraction. However, there was no formation of  $\text{C}_8$ ,  $\text{C}_{10+}$  or polyethylene (PE) in any of the catalytic systems.

**Table 1.** Ethylene oligomerization with  $\text{PNP}(\text{NR}_2)_2$ -based precatalysts 1–3 <sup>a</sup>.

Entry	Precatalyst	Activity $10^5 \text{ g}/(\text{molNi}\cdot\text{h})$	Product Distribution/%					
			$\text{C}_4$	$1\text{-C}_4$	<i>trans</i> - $\text{C}_4$	<i>cis</i> - $\text{C}_4$	$\text{C}_6$	$1\text{-C}_6$
1	1	103.0	84.3	34.6	26.2	23.5	15.7	3.0
2	2	76.9	88.1	30.4	30.1	27.6	11.9	1.8
3	3	10.9	69.9	16.8	32.9	20.2	30.1	0.6

<sup>a</sup> Reaction conditions: reaction pressure: 1.0 MPa; reaction time: 30 min; solvent: methylcyclohexane (20 mL); temperature: 45 °C; cocatalyst: EADC; precatalyst concentration: 0.6 mmol/L;  $n(\text{Al})/n(\text{Ni}) = 500:1$ .

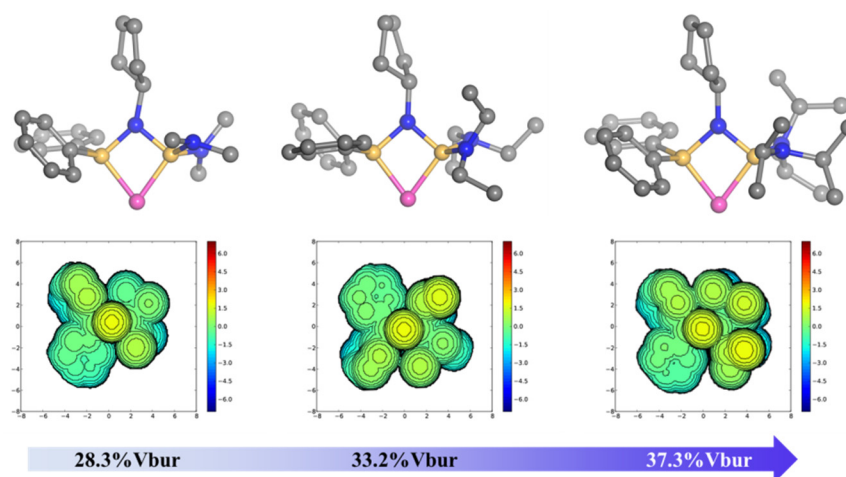


**Figure 1.** Structures of steric maps for precatalysts 1–3.

The effects of EADC, methylaluminumoxane (MAO), and modified methylaluminumoxane (MMAO) as different cocatalysts on the catalytic performance of precatalysts 1–3 were investigated and are presented in Table 2. All the cocatalysts successfully activated the precatalysts and presented the possibility of producing  $1\text{-C}_4$ . Compared to EADC (Table 2; entries 1, 4, and 7), less activity was observed when MAO or MMAO (Table 2; entries 2–3, 5–6, and 8–9) were used for the activation process, which could have been due to

the better stability of the chlorine atom in the EADC compared to the active species [19]. Therefore, EADC was suitable for the Ni-based PNP(NR<sub>2</sub>)<sub>2</sub> catalyst system. However, it is undeniable that MAO and MMAO as cocatalysts provided 100% C<sub>4</sub> selectivity, despite their low activity levels. How to maintain such high selectivity while improving the activity will be the focus of future research.

**Table 2.** Effects of the cocatalyst on precatalysts 1–3 on ethylene oligomerization <sup>a</sup>.

Entry	Precatalyst	Cocatalyst	Activity 10 <sup>5</sup> g/(molNi·h)	Product Distribution/%					
				C <sub>4</sub>	1-C <sub>4</sub>	<i>trans</i> -C <sub>4</sub>	<i>cis</i> -C <sub>4</sub>	C <sub>6</sub>	1-C <sub>6</sub>
1	1	EADC	103.0	84.3	34.6	26.2	23.5	15.7	3.0
2	1	MAO	1.7	100.0	36.3	32.3	31.4	—	—
3	1	MMAO	10.5	100.0	44.5	25.3	30.2	—	—
4	2	EADC	76.9	88.1	30.4	30.1	27.6	11.9	1.8
5	2	MAO	1.5	100.0	34.0	35.1	30.9	—	—
6	2	MMAO	3.5	100.0	39.1	33.6	27.3	—	—
7	3	EADC	10.9	69.9	16.8	32.9	20.2	30.1	0.6
8	3	MAO	0.1	100.0	35.5	34.5	30.0	—	—
9	3	MMAO	0.2	100.0	57.6	22.6	19.8	—	—

<sup>a</sup> Reaction conditions: reaction pressure: 1.0 MPa; reaction time: 30 min; solvent: methylcyclohexane (20 mL); temperature: 45 °C; precatalyst concentration: 0.6 mmol/L; cocatalyst: EADC; *n*(Al)/*n*(Ni) = 500:1.

Table 3 presents how increasing the catalyst's concentration from 0.3 to 1.2 mmol/L significantly increases catalytic activity at 0.6 mmol/L and exhibits a downward trend at 1.2 mmol/L.

**Table 3.** Effects of the precatalyst's concentration for precatalysts 1–3 on ethylene oligomerization <sup>a</sup>.

Entry	Precatalyst	Concentration mmol/L	Activity 10 <sup>5</sup> g/(molNi·h)	Product Distribution/%					
				C <sub>4</sub>	1-C <sub>4</sub>	<i>trans</i> -C <sub>4</sub>	<i>cis</i> -C <sub>4</sub>	C <sub>6</sub>	1-C <sub>6</sub>
1	1	0.3	54.6	82.1	29.2	26.9	26.0	17.9	0.8
2	1	0.6	103.0	84.3	34.6	26.2	23.5	15.7	3.0
3	1	1.2	87.4	83.4	36.8	25.9	20.7	16.6	3.8
4	2	0.3	2.1	100.0	60.2	39.8	—	—	—
5	2	0.6	76.9	88.1	30.4	30.1	27.6	11.9	1.8
6	2	1.2	52.8	86.0	37.6	27.1	21.3	14.0	1.6
7	3	0.3	0.1	100.0	44.8	55.2	—	—	—
8	3	0.6	10.9	69.9	16.8	32.9	20.2	30.1	0.6
9	3	1.2	7.5	91.9	21.1	47.7	23.1	8.1	1.4

<sup>a</sup> Reaction conditions: reaction pressure: 1.0 MPa; reaction time: 30 min; solvent: methylcyclohexane (20 mL); temperature: 45 °C; cocatalyst: EADC; *n*(Al)/*n*(Ni) = 500:1.

Previous studies reported that excessive catalyst loading may interfere with the catalytic environment of active species or limit the concentration of ethylene, which eventually leads to weakened catalytic activity [20,21]. For precatalyst 1, increasing the catalyst loading process was more conducive to the production of 1-C<sub>4</sub>, but the rising trend of C<sub>6</sub> was unfavorable for the high selectivity requirements of ethylene oligomerization (Table 3; entries 1–3). For precatalysts 2 and 3, the result of increased catalyst loading was similar to the result obtained for precatalyst 1. This may have been due to the fact that the metal active sites were better at accepting the insertion of ethylene into an environment containing a higher ethylene concentration to obtain excellent 1-C<sub>4</sub> selectivity (Table 3; entries 4 and 7), while the reason for the abrupt decline in its activity may have been due to the small quantity of cocatalyst corresponding to the molar ratio of the precatalyst, which was insufficient to remove the toxic impurities present in the system [4].

Table 4 shows the screening data for adjusting the *n*(Al)/*n*(Ni) ratio. Precatalysts 1–3 offered high catalytic activity when the *n*(Al)/*n*(Ni) ratio was 500 (Table 4; entries 2, 5, and 8). The inadequate ratio of *n*(Al)/*n*(Ni) may have led to a decline in the catalytic activity levels. This suggests that a lower or a higher concentration of EADC may affect

the activation, and possibly deactivation, of a catalytic system [4,22]. The greatest catalytic activity level of  $103.0 \times 10^5$  g/(molNi·h) was presented by precatalyst 1 at a ratio of 500 (Table 4; entry 2). Precatalysts 2 and 3 exhibited different oligomerization product-selectivity trends. Precatalyst 2 presented the highest C<sub>4</sub> selectivity value (90.5%) at a ratio of 300.

**Table 4.** Effects of  $n(\text{Al})/n(\text{Ni})$  ratio for precatalysts 1–3 on ethylene oligomerization <sup>a</sup>.

Entry	Precatalyst	$n(\text{Al})/n(\text{Ni})$	Activity 10 <sup>5</sup> g/(molNi·h)	Product Distribution/%					
				C <sub>4</sub>	1-C <sub>4</sub>	<i>trans</i> -C <sub>4</sub>	<i>cis</i> -C <sub>4</sub>	C <sub>6</sub>	1-C <sub>6</sub>
1	1	300	no	—	—	—	—	—	—
2	1	500	103.0	84.3	34.6	26.2	23.5	15.7	3.0
3	1	700	46.7	90.2	35.3	28.3	26.6	9.8	1.3
4	2	300	64.6	90.5	24.2	33.9	32.4	9.5	1.1
5	2	500	76.9	88.1	30.4	30.1	27.6	11.9	1.8
6	2	700	59.9	90.1	34.4	28.8	27.9	9.9	1.2
7	3	300	8.6	83.7	12.1	40.5	31.1	16.3	—
8	3	500	10.9	69.9	16.8	32.9	20.2	30.1	0.6
9	3	700	8.7	67.4	13.3	38.3	15.8	32.6	0.5

<sup>a</sup> Reaction conditions: reaction pressure: 1.0 MPa; reaction time: 30 min; solvent: methylcyclohexane (20 mL); temperature: 45 °C; precatalyst concentration: 0.6 mmol/L; cocatalyst: EADC.

High-temperature ethylene oligomerization provided the highest 1-C<sub>4</sub> selectivity value for precatalysts 1–3 (Table 5; entries 3, 5, and 9). However, higher or lower temperatures may affect the ethylene solubility performance of these catalytic systems, including catalyst decomposition [23,24]. Therefore, precatalysts 1 and 2 exhibited the highest catalytic activity at 45 °C (Table 5; entries 2 and 5), while precatalyst 3 presented the highest catalytic activity at 60 °C (Table 5; entry 8). The difference in the optimal temperature may have been due to the larger R-substituent of precatalyst 3, which can be explained by the slightly higher temperature required to promote the formation of active species. Consequently, it can be inferred that the catalytic performance of precatalysts 1–3 was strongly influenced by the reaction temperature [25].

**Table 5.** Effects of temperature for precatalysts 1–3 on ethylene oligomerization <sup>a</sup>.

Entry	Precatalyst	Temperature °C	Activity 10 <sup>5</sup> g/(molNi·h)	Product Distribution/%					
				C <sub>4</sub>	1-C <sub>4</sub>	<i>trans</i> -C <sub>4</sub>	<i>cis</i> -C <sub>4</sub>	C <sub>6</sub>	1-C <sub>6</sub>
1	1	30	52.0	90.4	23.3	50.8	16.3	9.6	2.1
2	1	45	103.0	84.3	34.6	26.2	23.5	15.7	3.0
3	1	60	46.9	90.3	36.3	27.2	26.8	9.8	1.3
4 <sup>b</sup>	2	30	10.1	69.7	26.1	29.4	14.2	30.3	—
5 <sup>b</sup>	2	45	59.9	90.1	34.4	28.8	27.9	9.9	1.2
6 <sup>b</sup>	2	60	48.4	89.9	33.2	28.9	27.8	10.1	1.6
7	3	45	10.9	69.9	16.8	32.9	20.2	30.1	0.6
8	3	60	16.5	81.5	16.6	46.4	18.5	18.5	1.1
9	3	90	12.5	78.5	26.1	27.0	25.4	21.5	0.6

<sup>a</sup> Reaction conditions: reaction pressure: 1.0 MPa; reaction time: 30 min; solvent: methylcyclohexane (20 mL); precatalyst concentration: 0.6 mmol/L; cocatalyst: EADC;  $n(\text{Al})/n(\text{Ni}) = 500:1$ ; <sup>b</sup>  $n(\text{Al})/n(\text{Ni}) = 700:1$ .

Crystallographic investigations revealed that precatalysts 1–3 adopted a mononuclear bidentate binding mode (Figure 2). Moreover, the steric constraints of its amine substituent on the P<sub>2</sub> atom may have affected the catalytic environment of the catalyst. The different steric-hindrance effects of amine substituents on the P<sub>2</sub> atom led to differences in the P<sub>1</sub>–Ni<sub>1</sub>–P<sub>2</sub> and N<sub>2</sub>–P<sub>2</sub>–N<sub>3</sub> angles. Compared to precatalysts 1 and 2, the larger P<sub>1</sub>–Ni<sub>1</sub>–P<sub>2</sub> and N<sub>2</sub>–P<sub>2</sub>–N<sub>3</sub> angles in precatalyst 3 hindered the coordination of inserted ethylene molecules with metal active centers, resulting in lower levels of activity and selectivity.

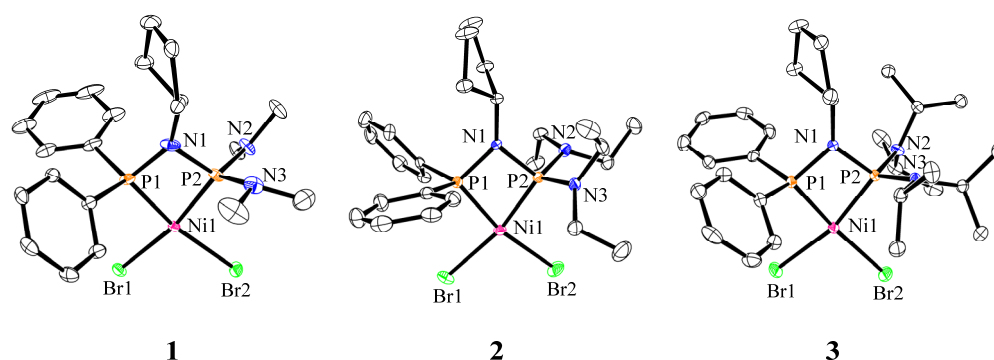


**Figure 2.** Molecular structures of complexes 1–3. Complex 1: Ni1–Br1 = 2.3512(5); Ni1–Br2 = 2.3236(5); Ni1–P1 = 2.1272(8); Ni1–P2 = 2.1278(9); P1–Ni1–P2 = 73.69(3); P1–N1–P2 = 98.0(1); N2–P2–N3 = 104.0(1). Complex 2: Ni1–Br1 = 2.3443(6); Ni1–Br2 = 2.3447(7); Ni1–P1 = 2.128(1); Ni1–P2 = 2.124(1); P1–Ni1–P2 = 73.51(5); P1–N1–P2 = 97.0(2); N2–P2–N3 = 103.9(2). Complex 3: Ni1–Br1 = 2.3486(5); Ni1–Br2 = 2.3411(5); Ni1–P1 = 2.1268(1); Ni1–P2 = 2.1531(1); P1–Ni1–P2 = 74.02(3); P1–N1–P2 = 97.6(1); N2–P2–N3 = 105.4(1).

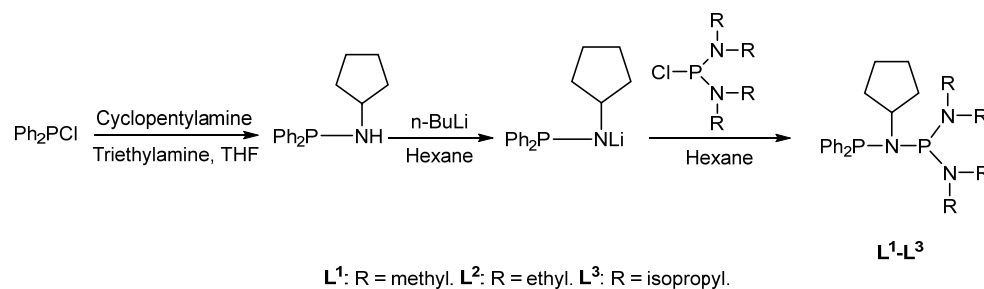
### 3. Materials and Methods

#### 3.1. General Information

All the experimental procedures were conducted in oven-dried flasks in a nitrogen atmosphere using the standard Schlenk technique or a purified N<sub>2</sub>-filled glove box. Anhydrous solvents were obtained using a multi-column purification system and further treated with suitable drying agents in a nitrogen atmosphere. All other reagents were purchased from Aldrich and used as received. A Bruker AscendIII-400 (Billerica, MA, USA) at 300 K was used to record the NMR spectra.

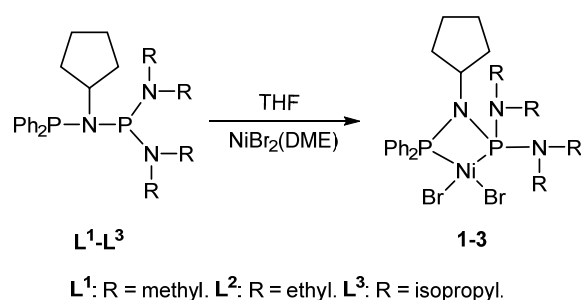
#### 3.2. Complex Preparation

The PNP(NR<sub>2</sub>)<sub>2</sub> ligands were synthesized according to reference (Scheme 1) [25].



**Scheme 1.** Synthesis of ligands L<sup>1</sup>–L<sup>3</sup>.

The nickel complexes were prepared as presented in Scheme 2. A solution of L<sup>1</sup> (0.0498 g, 0.105 mmol) in THF was added to the THF dispersion (10 mL) of NiBr<sub>2</sub>(DME) (0.0370 g, 0.1 mmol). The reaction mixture rapidly changed from orange to orange-red and was stirred for 8 h at room temperature. The solvent was vacuum evaporated, and then the orange, solid residue was washed three times with n-hexane. The solid was collected by filtration and then dried in a vacuum to obtain orange-colored complex 1 at an 80% yield. Complexes 2 and 3 were prepared using the same synthetic approach as complex 1, and orange-colored complexes were obtained at 81% and 85% yields, respectively. Slow diffusion of a CH<sub>2</sub>Cl<sub>2</sub> solution into n-hexane at –35 °C yielded single crystals for complexes 1–3. The results obtained for the molecular structures are presented in Figure 2 and Table S1 (Supplementary Materials). Single-crystal-structure data were submitted to the Cambridge Crystallographic Data Centre (CCDC) with deposition numbers 2106120–2106122 (corresponding to complexes 1–3). <sup>1</sup>H and <sup>31</sup>P NMR spectra of complexes 1–3 are presented in the Supplementary Materials (Figures S1–S6).



**Scheme 2.** Synthesis of nickel complexes 1–3 based on ligands L<sup>1</sup>–L<sup>3</sup>.

### 3.3. General Oligomerization Procedure

A 140 mL transparent glass reactor (Lab-Crest<sup>®</sup>) was heated in a high-temperature drying oven for 2 h at 105 °C before use. High-purity N<sub>2</sub> and ethylene were filled into the reactor three times. Subsequently, methylcyclohexane was injected into the reactor and heated to the reaction temperature. The cocatalyst and precatalyst were then injected into the reactor. The reactor was pressurized with ethylene to 1 MPa and the reaction continued for 30 min. The products were depressurized in an ice-water bath while the ethylene feed was turned off. The liquid phase was separated and analyzed by GC-FID (gas chromatography with a flame-ionization detector) using an Agilent 7890A with a HP-5 GC capillary column (Santa Clara, CA, USA), while heptane was used as an internal standard.

## 4. Conclusions

We reported on three nickel precatalysts with PNP(NR<sub>2</sub>)<sub>2</sub> ligands, which, upon activation with EADC, offered active and selective ethylene dimerization systems. Precatalyst 1, containing four methyl, was the most conducive to the active ethylene dimerization process, producing 83.4% C<sub>4</sub> (1-C<sub>4</sub> 36.8%) and up to 103.0 × 10<sup>5</sup> g/(molNi·h) activity under the appropriate conditions. The catalytic system of precatalyst 2 exhibited general activity (76.9 × 10<sup>5</sup> g/(molNi·h)) and greater C<sub>4</sub> selectivity (88.1%). The steric bulk of the R-substituents was observed to mainly influence the activity and slightly affect the selectivity of the catalysts. Moreover, the reaction conditions, such as catalyst loading, temperature, and n(Al)/n(Ni) ratio, were also identified as important parameters that influenced the catalytic performance. The single-crystal-analysis results may reveal the differences in the activity and selectivity of the three catalytic systems to some extent.

**Supplementary Materials:** The following are available online at <https://www.mdpi.com/article/10.3390/catal12091008/s1>, Figure S1: <sup>1</sup>H NMR Spectrum of complex 1 (CDCl<sub>3</sub>), Figure S2: <sup>31</sup>P NMR Spectrum of complex 1 (CDCl<sub>3</sub>), Figure S3: <sup>1</sup>H NMR Spectrum of complex 2 (CDCl<sub>3</sub>), Figure S4: <sup>31</sup>P NMR Spectrum of complex 2 (CDCl<sub>3</sub>), Figure S5: <sup>1</sup>H NMR Spectrum of complex 3 (CDCl<sub>3</sub>), Figure S6: <sup>31</sup>P NMR Spectrum of complex 3 (CDCl<sub>3</sub>), Table S1: Crystallographic Determination Parameters for 1–3 Complexes.

**Author Contributions:** Conceptualization, C.C. and T.J.; data curation, H.F.; formal analysis, C.C.; funding acquisition, C.C. and T.J.; investigation, J.Z. and J.M.; project administration, C.C.; supervision, T.J.; writing—original draft, H.F. and J.Z.; writing—review and editing, C.C. and H.F. All authors have read and agreed to the published version of the manuscript.

**Funding:** This research was funded by the National Natural Science Foundation of China (No. 22071178, 22050410271) and the PetroChina Innovation Foundation (No. 2019D-5007-0409).

**Data Availability Statement:** The data that supports the findings of this study are available in the supplementary material of this article.

**Conflicts of Interest:** The authors declare no conflict of interest.

## References

1. Boulens, P.; Pellier, E.; Jeanneau, E.; Reek, J.N.H.; Olivier-Bourbigou, H.; Breuil, P.A.R. Self-Assembled Organometallic Nickel Complexes as Catalysts for Selective Dimerization of Ethylene into 1-Butene. *Organometallics* **2015**, *34*, 1139–1142. [[CrossRef](#)]
2. Ngcobo, M.; Ojwach, S.O. Nickel(II) complexes chelated by N boolean AND N (benzimidazolylmethyl) amine ligands: Synthesis and catalytic behavior in tandem ethylene oligomerization and Friedel-Crafts alkylation reactions. *Inorg. Chim. Acta* **2017**, *467*, 400–404. [[CrossRef](#)]
3. Popeney, C.S.; Rheingold, A.L.; Guan, Z.B. Nickel(II) and Palladium(II) Polymerization Catalysts Bearing a Fluorinated Cyclophane Ligand: Stabilization of the Reactive Intermediate. *Organometallics* **2009**, *28*, 4452–4463. [[CrossRef](#)]
4. Huang, Y.W.; Zhang, L.; Wei, W.; Alam, F.; Jiang, T. Nickel-based ethylene oligomerization catalysts supported by PNSiP ligands. *Phosphorus Sulfur Silicon Relat. Elem.* **2018**, *193*, 363–368. [[CrossRef](#)]
5. Keim, W. Oligomerization of Ethylene to alpha-Olefins: Discovery and Development of the Shell Higher Olefin Process (SHOP). *Angew. Chem. Int. Ed* **2013**, *52*, 12492–12496. [[CrossRef](#)] [[PubMed](#)]
6. Kermagoret, A.; Braunstein, P. SHOP-type nickel complexes with alkyl substituents on phosphorus, synthesis and catalytic ethylene oligomerization. *Dalton Trans* **2008**, *2008*, 822–831. [[CrossRef](#)]
7. Kuhn, P.; Semeril, D.; Jeunesse, C.; Matt, D.; Neuburger, M.; Mota, A. Ethylene oligomerisation and polymerisation with nickel phosphanyl-enolates bearing electron-withdrawing substituents: Structure-reactivity relationships. *Chem. Eur. J.* **2006**, *12*, 5210–5219. [[CrossRef](#)]
8. Wang, S.L.; Sun, W.H.; Redshaw, C. Recent progress on nickel-based systems for ethylene oligo-/polymerization catalysis. *J. Organomet. Chem.* **2014**, *751*, 717–741. [[CrossRef](#)]
9. Olivier-Bourbigou, H.; Breuil, P.A.R.; Magna, L.; Michel, T.; Espada Pastor, M.F.; Delcroix, D. Nickel catalyzed olefin oligomerization and dimerization. *Chem. Rev.* **2020**, *120*, 7919–7983.
10. Feng, C.; Zhou, S.; Wang, D.; Zhao, Y.; Liu, S.; Li, Z.; Braunstein, P. Cooperativity in highly active ethylene dimerization by dinuclear nickel complexes bearing a bifunctional pn ligand. *Organometallics* **2021**, *40*, 184–193. [[CrossRef](#)]
11. Bekmukhamedov, G.E.; Sukhov, A.V.; Kuchkaev, A.M.; Yakhvarov, D.G. Ni-Based Complexes in Selective Ethylene Oligomerization Processes. *Catalysts* **2020**, *10*, 498. [[CrossRef](#)]
12. Ajjallal, N.; Kuhn, M.C.A.; Boff, A.D.G.; Horner, M.; Thomas, C.M.; Carpentier, J.F.; Casagrande, O.L. Nickel complexes based on tridentate pyrazolyl ligands for highly efficient dimerization of ethylene to 1-butene. *Organometallics* **2006**, *25*, 1213–1216. [[CrossRef](#)]
13. Gutsulyak, D.V.; Gott, A.L.; Piers, W.E.; Parvez, M. Dimerization of Ethylene by Nickel Phosphino-Borate Complexes. *Organometallics* **2013**, *32*, 3363–3370. [[CrossRef](#)]
14. Xu, C.J.; Shen, Q.; Sun, X.L.; Tang, Y. Synthesis, Characterization, and Highly Selective Ethylene Dimerization to 1-Butene of [O-NX]Ni(II) Complexes. *Chin. J. Chem* **2012**, *30*, 1105–1113. [[CrossRef](#)]
15. Meng, X.J.; Zhang, L.; Chen, Y.H.; Jiang, T. Silane-bridged diphosphine ligands for nickel-catalyzed ethylene oligomerization. *React. Kinet. Mech. Cat.* **2016**, *119*, 481–490. [[CrossRef](#)]
16. Wang, J.D.; Alam, F.; Chang, Q.Q.; Chen, Y.H.; Jiang, T. Catalytic behavior tuning via structural modifications of silylated-diphosphine Ni(II) complexes for ethylene selective dimerization. *Appl. Organomet. Chem.* **2020**, *34*, e5722. [[CrossRef](#)]
17. Falivene, L.; Cao, Z.; Petta, A.; Serra, L.; Poater, A.; Oliva, R.; Scarano, V.; Cavallo, L. Towards the online computer-aided design of catalytic pockets. *Nat. Chem.* **2019**, *11*, 872–879. [[CrossRef](#)]
18. Wei, W.; Yu, B.W.; Alam, F.; Huang, Y.W.; Cheng, S.L.; Jiang, T. Ethylene oligomerization promoted by nickel-based catalysts with silicon-bridged diphosphine amine ligands. *Transit. Met. Chem* **2018**, *44*, 125–133. [[CrossRef](#)]
19. de Oliveira, L.L.; Campedelli, R.R.; Kuhn, M.C.A.; Carpentier, J.F.; Casagrande, O.L. Highly selective nickel catalysts for ethylene oligomerization based on tridentate pyrazolyl ligands. *J. Mol. Catal. A Chem.* **2008**, *288*, 58–62. [[CrossRef](#)]
20. Do, L.H.; Labinger, J.A.; Bercaw, J.E. Spectral Studies of a Cr(PNP)-MAO System for Selective Ethylene Trimerization Catalysis: Searching for the Active Species. *Acc Catal.* **2013**, *3*, 2582–2585. [[CrossRef](#)]
21. Alam, F.; Zhang, L.; Wei, W.; Wang, J.D.; Chen, Y.H.; Dong, C.H.; Jiang, T. Catalytic Systems Based on Chromium(III) Silylated-Diphosphinoamines for Selective Ethylene Tri-/Tetramerization. *Acc Catal.* **2018**, *8*, 10836–10845. [[CrossRef](#)]
22. Wang, T.; Dong, B.; Chen, Y.H.; Mao, G.L.; Jiang, T. Nickel complexes incorporating pyrazole-based ligands for ethylene dimerization to 1-butylene. *J. Organomet. Chem.* **2015**, *798*, 388–392. [[CrossRef](#)]
23. Zhang, N.; Wang, J.M.; Huo, H.L.; Chen, L.D.; Shi, W.G.; Li, C.Q.; Wang, J. Iron, cobalt and nickel complexes bearing hyperbranched iminopyridyl ligands: Synthesis, characterization and evaluation as ethylene oligomerization catalysts. *Inorg. Chim. Acta* **2018**, *469*, 209–216. [[CrossRef](#)]
24. Guo, C.Y.; Xu, H.; Zhang, M.G.; Zhang, X.H.; Yan, F.W.; Yuan, G.Q. Immobilization of bis(imino)pyridine iron complexes onto mesoporous molecular sieves and their catalytic performance in ethylene oligomerization. *Catal. Commun.* **2009**, *10*, 1467–1471. [[CrossRef](#)]
25. Zhang, J.Y.; Alam, F.; Fan, H.N.; Ma, J.; Jiang, T. Chromium catalysts based on PNP(NR<sub>2</sub>)<sub>2</sub> ligands for selective ethylene oligomerization. *Appl. Organomet. Chem.* **2022**, *36*, e6454. [[CrossRef](#)]